Pramana – J. Phys. (2020) 94:129
https://doi.org/10.1007/s12043-020-01996-9

Viscous Ricci dark energy model with matter creation: Exact solution and observational tests

AJAY KUMAR and C P SINGH*

Department of Applied Mathematics, Delhi Technological University, Delhi 110 042, India
*Corresponding author. E-mail: cpsingh@dce.ac.in

MS received 22 April 2020; accepted 18 June 2020

Abstract. In this paper, the dissipative mechanism (bulk viscosity and matter creation) is introduced to describe the effects of cosmic non-perfect fluid on the Ricci dark energy (RDE) model. We consider matter creation and bulk viscosity as two independent irreversible processes. Assuming suitable forms of the bulk viscous coefficient and matter creation rate, we find the exact solution of the field equations. We carry out fitting analysis on the cosmological parameters in the model by using Type Ia supernovae data, observational Hubble data and baryon acoustic oscillation (BAO) data with cosmic microwave background. We plot the trajectory of cosmological parameters with the best-fit values of model parameters and discuss all possible (deceleration, acceleration and their transitions) evolutions of the model. The current values of deceleration parameter and equation of state parameter are found to be $q_0 = -0.362$ and $\omega_{\text{eff}} = -0.575$, respectively. The age of the Universe is found to be $t_0 \simeq 13.397$ Gyr, which is very close to the ΛCDM model. We further discuss the geometrical diagnostic parameters such as statefinder and Om to distinguish the model with ΛCDM model. Finally, we discuss the behaviour of energy conditions for our model and find that the model satisfies the null energy condition (NEC), weak energy condition (WEC) and dominant energy condition (DEC) while it violates strong energy condition (SEC).

Keywords. Holographic dark energy cosmology; bulk viscosity; matter creation.

PACS Nos **95.36.+x; 98.80.−k**

1. Introduction

The study of accelerated expansion of the present Universe becomes one of the vital topics in cosmology during the last few years [1–3]. This fact is widely confirmed by the recent observational data. Many theories are considered to get a proper explanation of this phenomenon. These observations lead to a new kind of matter which violates the strong energy condition (SEC), i.e., $\rho + 3p < 0$. The energy density of matter responsible for such a condition to be satisfied at a certain stage of evolution of the Universe is referred to as dark energy (DE). Various theories have been proposed to explain DE problems [4–12]. The simplest DE model which is based on cosmological constant is dubbed ΛCDM model [13]. However, this model suffers from two problems called fine-tuning and coincidence problems.

Based on holographic principle [14], Li [15] proposed a new DE model called holographic dark energy (HDE) model in which the DE density was considered as $\rho_d = 3b^2 M_P^2 L^{-2}$, where b^2 is a dimensionless constant, $M_P^{-2} = G$ is the Planck mass and L denotes the infrared (IR) cut-off. It was found that the HDE with Hubble horizon as its IR cut-off does not give an accelerating Universe. Later on, he considered the future event horizon of the Universe as the infrared cut-off. This HDE model is able to explain the accelerated expansion of the Universe which fits the current observations. In the recent past, several works [16–21] have been carried out in HDE models to describe the accelerating behaviour of the Universe. Gao *et al* [22] suggested that the DE density might be inversely proportional to the Ricci scalar curvature, R, and they called this model the Ricci dark energy (RDE) model. In RDE model, the future event horizon has been replaced by the inverse of the Ricci scalar curvature. This model not only avoids the causality problem and is phenomenologically viable, but also solve the coincidence problem. They introduced HDE density proportional to the Ricci scalar, i.e., $\rho_d \propto R$, where $R = -6(2H^2 + \dot{H} +$

Published online: 20 August 2020

$\frac{k}{a^2}$). Thus, the energy density of the RDE model in a flat Friedmann–Robertson–Walker (FRW) Universe is given by

$$\rho_d = 3\alpha(\dot{H} + 2H^2), \tag{1}$$

where α is a dimensionless parameter, H is the Hubble parameter and $\dot{H}$ represents the derivative of the Hubble parameter with respect to the cosmic time t. This model fits with the observational data and well explain the coincidence problem also. In [23–26], researchers have shown that the RDE is suitable for describing the current acceleration of the Universe.

It is well known that the content of the Universe as a perfect fluid is assertive as it suggests no dissipation, which actually exists widely, and intuitively plays an important role in the evolution of the Universe. To be more realistic, the Universe is assumed to be filled with dissipative media. Therefore, cosmology based on imperfect fluid is proposed reasonably. Viscosity is a concept in fluid mechanics which is related to an exotic fluid with some thermodynamical features such as bulk and/or shear viscosities. In cosmology, shear viscosity is related to the anisotropy of the space–time whereas the bulk viscosity is usually related to the isotropic Universe. To reduce the equilibrium pressure in an expanding Universe, bulk viscosity can be useful. In cosmology, the viscosity concept was first discussed by Misner [27]. Several researchers [28–43] have discussed the effect of bulk viscosity to understand the DE phenomenon.

The study of matter creation in the relativistic cosmological models has drawn the attention of a number of researchers. In the framework of general relativity (GR), the adiabatic irreversible matter creation was first studied by Prigogine *et al* [44,45]. In their papers, they discussed that the second law of thermodynamics may be modified to accommodate flow of energy from gravitational field to the created matter field. This phenomenon of matter creation has been studied by many researchers in detail within the context of standard GR [46–54]. In the context of the recent acceleration, the concept of irreversible particle creation has been reconsidered due to its capability to produce an effective negative pressure. For more details, the reader is referred to refs [55–65]. Prigogine *et al* [44,45] considered the viscous and matter creation processes as two independent processes. Some researchers [35,66–68] have studied theses two dissipative processes by considering two independent phenomena.

In this paper, we study the effects of bulk viscosity and adiabatic matter creation in RDE model within the framework of FRW Universe. We discuss the evolution of the Universe by constraining the model parameters through combined observational data. We plot the trajectory of Hubble parameter and ΛCDM with error bar from Hubble data. We study the dynamical properties of our model by calculating the deceleration parameter, jerk, snap and lerk parameters analytically and geometrically. We further discuss the statefinder and Om diagnostics to discriminate RDE model with other standard DE models. We also discuss the behaviour of energy conditions for the RDE model.

This paper is organised as follows: In §2, we present the Einstein field equations with bulk viscosity and matter creation for RDE model in the framework of a flat FRW line element. In §3, we obtain exact solution to the field equations to obtain the Hubble parameter and the scale factor. We fit the model to the combined data set of Type Ia Supernovae, observational Hubble data and combined data of baryon acoustic oscillations and cosmic microwave background, and present the fitting results in §4. Many interesting issues including the age of the Universe are discussed in §5. We compare RDE model with other DE models by calculating statefinder parameters, Om diagnostics and cosmographic parameters in §6. In §7, we discuss the energy conditions for our model. Finally, we summarise our results in §8. It is to be noted that we have used matter creation and particle creation synonymously throughout the article.

2. The cosmological model

We consider a homogeneous and isotropic flat Friedmann–Robertson–Walker (FRW) line element with the units $8\pi G = 1$ and $c = 1$

$$\mathrm{d}s^2 = \mathrm{d}t^2 - a^2(t)[\mathrm{d}r^2 + r^2(\mathrm{d}\theta^2 + \sin^2\theta\,\mathrm{d}\phi^2)], \tag{2}$$

where r, θ and ϕ are dimensionless co-moving coordinates and $a(t)$ is the scale factor. The Einstein's field equations (EFE) take the usual form

$$R_{\mu\nu} - \frac{1}{2}g_{\mu\nu}R = -T_{\mu\nu}, \tag{3}$$

where $T_{\mu\nu}$ is the energy–momentum tensor for the perfect fluid which modifies due to particle creation in adiabatic irreversible open thermodynamic systems and bulk viscous stress. We assume that the Universe is filled with pressureless dark matter and the energy of RDE for which the energy–momentum tensor is given by [68–70]

$$T_{\mu\nu} = (\rho_m + \rho_d + p_{\mathrm{eff}})u_\mu u_\nu - p_{\mathrm{eff}}g_{\mu\nu}. \tag{4}$$

Here, ρ_m and ρ_d denote the energy densities of dark matter and RDE, respectively, and p_{eff} is the effective pressure

$$p_{\mathrm{eff}} = p_d + p_c + p_v, \tag{5}$$

where p_d is the pressure of RDE, p_c is the pressure associated with the creation of particle out of the gravitational field [44,45] and p_v represents the viscous pressure which is assumed as $p_v = -3\zeta H$, where ζ is the bulk viscous coefficient [71]. The bulk viscous pressure, p_v, represents only a small correction to the thermodynamical pressure; it is a reasonable assumption that the inclusion of viscous term in the energy–momentum tensor does not fundamentally change the dynamics of the cosmic evolution. The pressure and density of RDE are related by the equation of state (EoS) $p_d = \omega_d \rho_d$, where ω_d is the EoS parameter of RDE.

In the background of metric (2) in the general theory of relativity, EFEs (3) yield the following two independent equations:

$$3H^2 = \rho_m + \rho_d, \tag{6}$$

$$2\dot{H} + 3H^2 = -p_{\text{eff}} = -(p_d + p_c - 3\zeta H), \tag{7}$$

where $H = \dot{a}/a$ is the Hubble parameter which measures the fractional rate of change of the scale factor $a(t)$ and the overhead dot indicates the derivative with respect to the cosmic time t.

In the presence of a gravitational particle source, the number of fluid particles is not conserved, i.e., $N^{\mu}_{;\mu} \neq 0$, where $N = nV$ is the total number of particles in a system. It means that N is variable, i.e., the system is open. Here, n is the particle number density and $V = a^3$ is the volume of the system. The particle number density flow $N^{\mu} = nu^{\mu}$ is assumed to satisfy the balance equation [68]

$$\dot{n} + 3Hn = n\Gamma, \tag{8}$$

where Γ denotes the particle creation rate of cold dark matter. Equation (8), when combined with the second law of thermodynamics, naturally leads to the appearance of a negative pressure directly associated with the rate Γ and the creation pressure p_c, which adds to the other pressures (i.e., of radiation, baryons, DM and vacuum pressure) in the total energy–momentum tensor. As should be expected, the creation pressure is defined in terms of the creation rate and other physical quantities. In the case of adiabatic creation of DM, it is given by [46–50,52]

$$p_c = -\frac{\rho_m}{3H}\Gamma. \tag{9}$$

It is clear from the above equation that if the creation pressure p_c is negative, then it may drive the era of cosmic acceleration of the Universe. We have $p_c < 0$, when $\Gamma > 0$ since $\rho_m > 0$ and $H > 0$, i.e. $\dot{a} > 0$, and $p_c > 0$ when $\Gamma < 0$. Let us now assume the particle creation rate Γ to discuss the RDE model. The most natural choice is taken to be [51]

$$\Gamma = 3\beta H, \tag{10}$$

where β is a constant parameter which lies in the interval $0 \leq \beta < 1$. It has been found that this form of Γ does not favour the epoch in the evolution of the Universe. Lima *et al* [53] have investigated the CDM model with this form of Γ, but time-dependent dimensionless parameter β. However, we restrict ourself with β as a constant but study with the other dissipative mechanism, i.e., viscous fluid to find the epoch of the evolution of the Universe. We consider that these two dissipative mechanisms have independent physical phenomena.

Now, using (10) into (9), we obtain

$$p_c = -\beta\rho_m. \tag{11}$$

Using (10) into (8), we find the solution for the particle number density as

$$n = n_0\left(\frac{a_0}{a}\right)^{3(1-\beta)}, \tag{12}$$

where n_0 is the constant of integration and considered as the present value of particle number density. In adiabatic particle production, the particles and entropy are produced in the space–time, but the specific entropy (per particle) $\sigma = S/N$, remains constant. This implies that $\dot{S}/S = \dot{N}/N$.

Using (1) and (11), a single evolution equation from (6) and (7) can be obtained as

$$[2 + 3\alpha(\beta + \omega_d)]\dot{H} + 3[1 - \beta + 2\alpha(\beta + \omega_d)] H^2 - 3\zeta H = 0. \tag{13}$$

In the absence of bulk viscosity and matter creation, i.e., taking $\zeta = 0$ and $\beta = 0$, the solution of (13) for RDE model is given by

$$H = H_0\left(\frac{a_0}{a}\right)^{l}, \tag{14}$$

where a_0 and H_0 are respectively the present-day values of the scale factor and Hubble parameter at time t_0 and $l = 3(1+2\alpha\omega_d)/(2+3\alpha\omega_d)$. The solution of the scale factor is obtained as

$$a = a_0\,[1 + lH_0(t - t_0)]^{1/l}\,. \tag{15}$$

The scale factor shows the power-law expansion. The deceleration parameter, which is defined as $q = -a\ddot{a}/\dot{a}^2$, gives $q = (l - 1)$. Thus, the value of q is constant. Therefore, the RDE model itself does not describe the transition redshift.

Further, let us consider the RDE model with matter creation in the absence of bulk viscosity, i.e., $\zeta = 0$. The solution of (13) in the presence of matter creation is given by

$$H = H_0\left(\frac{a_0}{a}\right)^{k}, \tag{16}$$

where $k = 3[1 - \beta + 2\alpha(\beta + \omega_d)]/[2 + 3\alpha(\beta + \omega_d)]$. The solution of the scale factor is given by

$$a = a_0 \left(1 + k H_0 (t - t_0)\right)^{1/k}. \tag{17}$$

Equation (17) again shows that the expansion of the Universe is of power-law form. The constant value of $q = (k - 1)$ shows that the model does not transit from decelerated phase to accelerated phase. The model decelerates for $k > 1$, has marginal inflation at $k = 1$ and accelerates for $k < 1$. Therefore, the form of Γ defined in eq. (10) does not explain the present-day Universe, i.e., the transition phase in the absence of bulk viscosity.

In what follows, we find the solution of eq. (13) with non-zero bulk viscosity and matter creation by assuming suitable form of bulk viscous coefficient, ζ.

3. Solution with viscosity and matter creation

Following [72–74], we consider ζ of the following form:

$$\zeta = \zeta_0 + \zeta_1 H, \tag{18}$$

where ζ_0 and ζ_1 are positive constants. Equation (18) represents the general assumption as it is a combination of two forms, $\zeta = \zeta_0$ and $\zeta \propto H$. This motivation can be traced in fluid mechanics where the transport/viscosity phenomenon is involved with velocity $\dot{a}$ which is related to the expansion rate H. We define the dimensionless bulk viscous coefficients ξ, ξ_0 and ξ_1 as

$$\xi = \frac{\zeta}{H_0}, \quad \xi_0 = \frac{\zeta_0}{H_0} \quad \text{and} \quad \xi_1 = \zeta_1, \tag{19}$$

where H_0 is the current value of the Hubble parameter. Using the above transformation in (18), we obtain the dimensionless form of bulk viscosity as $\xi = \xi_0 + \xi_1 h$, where $h = H/H_0$ is the dimensionless Hubble parameter.

Using the relation

$$\frac{\mathrm{d}}{\mathrm{d}t} = \frac{\dot{a}}{a}\frac{\mathrm{d}}{\mathrm{d}\ln a}$$

in (13), a dimensionless evolution equation for $h = H/H_0$ is given by

$$\psi_2 h' + 3\psi_1 h - 3\xi_0 = 0, \tag{20}$$

where $\psi_1 = [1 - \beta - \xi_1 + 2\alpha(\beta + \omega_d)]$, $\psi_2 = [2 + 3\alpha(\beta + \omega_d)]$ and the prime denotes the differentiation with respect to the conformal time $\ln a$.

Integration of eq. (20) gives

$$h(a) = \frac{\xi_0}{\psi_1} + \left(1 - \frac{\xi_0}{\psi_1}\right)\left(\frac{a}{a_0}\right)^{-3\psi_1/\psi_2}, \quad \psi_1 \neq 0. \tag{21}$$

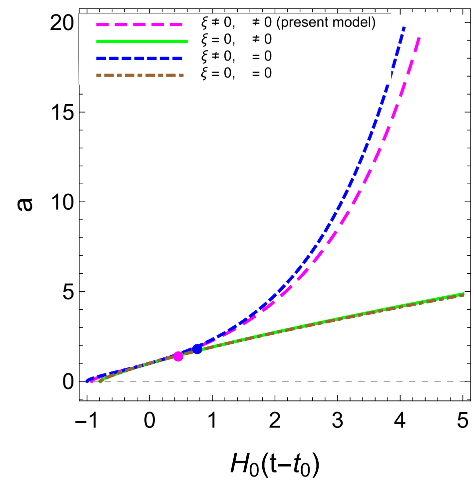

Figure 1. The evolution of the scale factor with respect to $H_0(t - t_0)$ for the best-fit values of free parameters. The dot denotes the transition value. The brown and green trajectories of the scale factor show decelerated expansion whereas the blue and magenta trajectories show the accelerated expansion after the transition point.

Now, using the relation $(a_0/a) = (1 + z)$, we can write the Hubble parameter H in terms of redshift z as

$$H(z) = H_0\left[\frac{\xi_0}{\psi_1} + \left(1 - \frac{\xi_0}{\psi_1}\right)(1 + z)^{3\psi_1/\psi_2}\right]. \tag{22}$$

We derive the t–z relationship, which comes out as

$$t(z) = t_0 + \frac{\psi_2}{3\xi_0 H_0}\ln\left[1 + \frac{\xi_0}{\psi_1}\{(1 + z)^{-3\psi_1/\psi_2} - 1\}\right]. \tag{23}$$

From (22), the scale factor $a(t)$ is obtained as

$$a(t) = a_0\left[1 + \frac{\psi_1}{\xi_0}\left(\mathrm{e}^{\frac{3\xi_0 H_0(t - t_0)}{\psi_2}} - 1\right)\right]^{\psi_2/3\psi_1}, \quad \xi_0 \neq 0, \quad \psi_1 \neq 0, \tag{24}$$

where a_0 is the scale factor at the present epoch and now onwards can be taken as 1. To better understand the evolution of the scale factor, we have plotted the graph of $a(t)$ with respect to $H_0(t - t_0)$ in figure 1 for the best-fitted values of the model parameters. The best-fit values of the model parameters from the observations are given in table 1 (discussed in §4). From figure 1, it is observed that the accelerated expansion starts earlier in the RDE model with bulk viscosity and matter creation (violet trajectory) than the RDE model with bulk viscosity (blue trajectory) during the evolution of the Universe.

The Hubble parameter $H(t)$ in terms of t can be written as

$$H(t) = H_0 \mathrm{e}^{\frac{3\xi_0 H_0(t - t_0)}{\psi_2}}\left[1 + \frac{\psi_1}{\xi_0}\left(\mathrm{e}^{\frac{3\xi_0 H_0(t - t_0)}{\psi_2}} - 1\right)\right]^{-1}.$$

Table 1. The best-fit values of the free parameters of RDE model with bulk viscosity and matter creation using SNe + OHD + BAO/CMB samples

Parameters	Best-fit values
ξ_0	5.223
ξ_1	0.485
β	0.777
ω_d	−0.240
α	8.078
M	24.95
χ^2_{min}	58.79
χ^2_{red}	0.77

(25)

The effective dark energy density, ρ_{eff}, and effective pressure, p_{eff}, are respectively given as

$$\rho_{\text{eff}} = 3H_0^2 \mathrm{e}^{\frac{6\xi_0 H_0(t-t_0)}{\psi_2}} \left[1 + \frac{\psi_1}{\xi_0}\left(\mathrm{e}^{\frac{3\xi_0 H_0(t-t_0)}{\psi_2}} - 1\right)\right]^{-2} \tag{26}$$

and

$$p_{\text{eff}} = -\frac{3H_0^2\xi_0 \mathrm{e}^{\frac{3\xi_0 H_0(t-t_0)}{\psi_2}}\left[\psi_2 \mathrm{e}^{\frac{3\xi_0 H_0(t-t_0)}{\psi_2}} + 2(\xi_0 - \psi_1)\right]}{\psi_2\left[1 + \frac{\psi_1}{\xi_0}(\mathrm{e}^{\frac{3\xi_0 H_0(t-t_0)}{\psi_2}} - 1)\right]^2}. \tag{27}$$

4. Parameters estimation

We use the Hubble parameter obtained in eq. (22) and estimate the best fit of the model parameters $\xi_0, \xi_1, \beta, \omega_d$ and α using the combined data set, consisting of the Type Ia supernova (SNe) data set, observational Hubble data (OHD) and the combined baryon acoustic oscillation (BAO) and cosmic microwave background (CMB) data. In order to figure out the observational constraints, we employ the publicly available EMCEE codes [75] for implementing the Markov chain Monte Carlo (MCMC) method. We choose the current Hubble constant value as $H_0 = 67.8$ km/s/Mpc from Planck 2015 results [76].

It is believed that the SNe observation provides the evidence of cosmic accelerating expansion. For this purpose, we used 31 binned data points of the cJLA data set with the range $0.01 < z < 1.3$ [77] for which χ^2 is defined by

$$\chi^2_{\text{SNe}} = r^t C_b^{-1} r, \tag{28}$$

where $r = \mu_b - M - 5\log_{10} d_L$. Here μ_b is the observational distance modulus for a supernova at redshift z, M is a free normalisation parameter and C_b is the covariance matrix of μ_b for which see table F.2 in [77]. In the above equation, d_L is the luminosity distance which is defined by

$$d_L = \frac{c(1+z)}{H_0}\int_0^z \frac{\mathrm{d}z'}{H(z',\theta)}, \tag{29}$$

where c is the speed of light and θ is the representation of model parameters α, β, ω_d, ξ_0 and ξ_1.

In the recent past, the measurement of Hubble parameter $H(z)$ got much attention from the researchers due to its model-independent nature. In this paper, we compare our model with 43 data points of the Hubble parameter in the red-shift range $0 < z < 2.5$ [78]. The χ^2 function is defined as follows:

$$\chi^2_{\text{OHD}} = \sum_{i=1}^{n} \frac{[H(z_i) - H_{\text{obs}}(z_i,\theta)]^2}{\sigma_i^2}, \tag{30}$$

where $H(z_i)$ and $H_{\text{obs}}(z_i,\theta)$ represent the theoretical and observed values of Hubble parameter, respectively. The standard deviation in the observed value is denoted by σ_i.

We consider BAO and CMB data, i.e., BAO/CMB data from different observational missions [79]. We combine the sample of BAO distance measurements from SDSS(R) [80], isotropic BAO measurement of 6dF Galaxy survey [81], BOSS CMASS [82] and three parallel measurements from WiggleZ survey [83] as the latest observational data for BAO. We combine these results with the Planck 2015 results [84].

In the context of BAO, the angular diameter, $d_A(z,\theta)$ is defined as

$$d_A(z_*,\theta) = c\int_0^{z_*} \frac{\mathrm{d}z'}{H(z',\theta)}, \tag{31}$$

where z_* indicates the photon decoupling redshift and holds the value $z_* = 1090$ as per the Planck 2015 results [84]. $D_v(z,\theta)$ represents the dilation scale which is given by

$$D_v(z,\theta) = \left(\frac{d_A^2(z,\theta)cz}{H(z,\theta)}\right)^{1/3}.$$

The distant redshift d_z is given by

$$d_z = \frac{r_s(z_*)}{D_v(z)}, \tag{32}$$

where $r_s(z_*)$ is defined as the co-moving sound horizon at the time when photons decouple, which is assumed to be the same as it is considered in ref. [79].

The χ^2 function can be explained as [79]

$$\chi^2_{\text{BAO/CMB}} = A^T C^{-1} A, \tag{33}$$

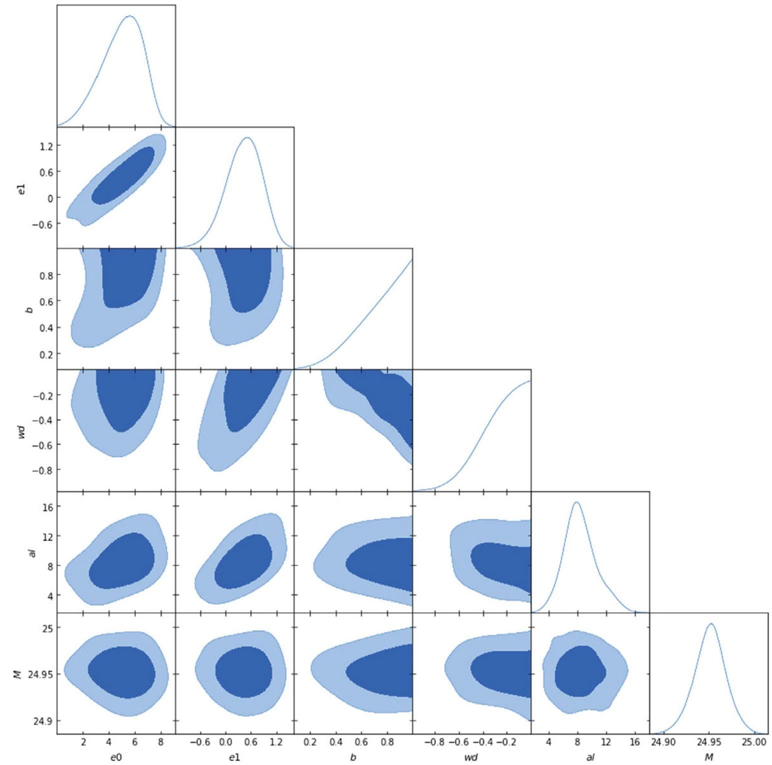

Figure 2. The contour plot for the free parameters using the observational data SNe + OHD + BAO/CMB for RDE model with bulk viscosity and matter creation. The labels *e*0, *e*1, *b*, *wd* and *al* denote ξ_0, ξ_1, β, ω_d and α parameters, respectively.

where A is the matrix

$$A = \begin{bmatrix} \dfrac{d_A(z_*,\theta)}{D_v(0.106,\theta)} - 30.84 \\ \dfrac{d_A(z_*,\theta)}{D_v(0.35,\theta)} - 10.33 \\ \dfrac{d_A(z_*,\theta)}{D_v(0.57,\theta)} - 6.72 \\ \dfrac{d_A(z_*,\theta)}{D_v(0.44,\theta)} - 8.41 \\ \dfrac{d_A(z_*,\theta)}{D_v(0.6,\theta)} - 6.66 \\ \dfrac{d_A(z_*,\theta)}{D_v(0.73,\theta)} - 5.43 \end{bmatrix}$$

C^{-1} is the inverse of the covariance matrix [79]. We have taken the correlation coefficient from ref. [85].

Considering these cosmological data sets together, i.e. (SNe + OHD + BAO/CMB), the total χ^2 function is then given by

$$\chi^2 = \chi^2_{\text{SNe}} + \chi^2_{\text{OHD}} + \chi^2_{\text{BAO/CMB}}. \tag{34}$$

The best-fit values for the model parameters obtained by minimising total χ^2 are given in table 1 and the contour plot is shown in figure 2 with 1σ (68.3%) and 2σ (95.4%) confidence level.

5. Evolution of cosmological parameters

The Hubble parameter in eq. (21) shows a decreasing behaviour with the scale factor. It can have infinitely large value in the early stages and decreases as the Universe expands and finally saturated to a constant value as $a \to \infty$. Figure 1 shows the behaviour of the scale factor with cosmic time. The transition point is found to be $a_{\text{tr}} = 0.936$ where the model transits from decelerated phase to accelerated phase.

The deceleration parameter q is a geometric parameter which measures the state of acceleration/deceleration of the Universe. The positive value of q represents the decelerated phase of the Universe whereas the negative value represents the accelerated phase. Using (24), we obtain

$$q(t) = -1 + \frac{3(\psi_1 - \xi_0)}{\psi_2} \mathrm{e}^{\frac{-3\xi_0 H_0(t-t_0)}{\psi_2}}. \tag{35}$$

Thus, the deceleration parameter (DP) in terms of z can be obtained as

$$q(z) = -1 + \frac{3(\psi_1 - \xi_0)}{\psi_2}\left[\frac{\psi_1}{\psi_1 + \xi_0\{(1+z)^{-3\psi_1/\psi_2} - 1\}}\right]. \tag{36}$$

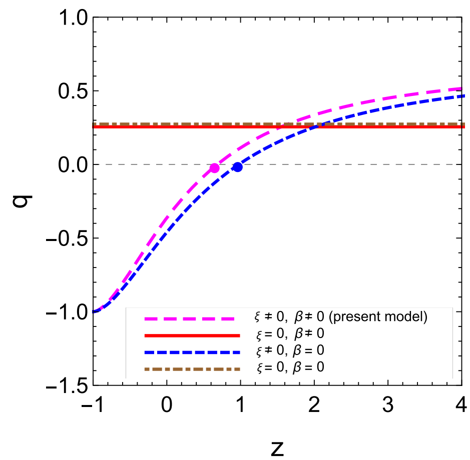

Figure 3. The q–z relation diagram for the best-fitted model parameters. The dot denotes the transition point from where the model transits from decelerated phase to accelerated phase. The horizontal orange and grey trajectories show the constant deceleration values whereas the transition trajectories (blue and violet) are due to the RDE model with bulk viscosity, and the RDE model with bulk viscosity and matter creation, respectively.

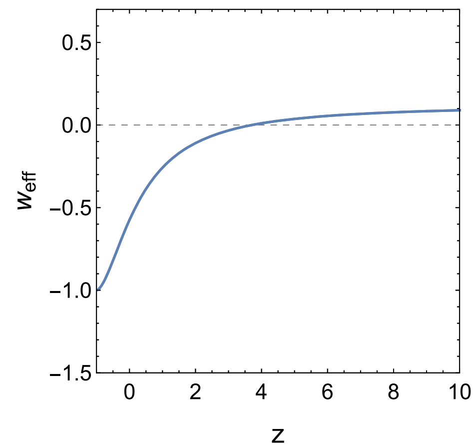

Figure 4. The $\omega_{\rm eff}$–z relation diagram for the best-fitted model parameters.

The present value of deceleration parameter, q_0, corresponding to $z = 0$ is given by

$$q_0 = -1 + \frac{3(\psi_1 - \xi_0)}{\psi_2}. \tag{37}$$

For best-fit value of parameters, $q_0 = -0.362$, is higher than the corresponding WMAP value $q_0 = -0.60$ [86]. In figure 3 we plot the deceleration parameter $q(z)$ against cosmic redshift z for best fitted values of RDE model. It is observed that q changes its sign from positive to negative showing the transition from decelerated phase to accelerated phase. The transition redshift, $z_{\rm tr}$, is found to be $z_{\rm tr} = 0.68$ for the RDE model, which is within the range of the transition redshift $z_{\rm tr} = 0.45$–0.73 in the concordance ΛCDM model [87].

We can obtain the effective equation of state (EoS) parameter, $\omega_{\rm eff}$, using the standard relation

$$\omega_{\rm eff} = -1 - \frac{1}{3}\frac{2a}{h}\frac{{\rm d}h}{{\rm d}a}$$

as

$$\omega_{\rm eff} = -1 + \frac{2(\psi_1 - \xi_0)}{\psi_2}\left[\frac{\psi_1}{\psi_1 + \xi_0\{(1+z)^{-3\psi_1/\psi_2} - 1\}}\right]. \tag{38}$$

It can be observed that in the late-time as $z \to -1$, $\omega_{\rm eff} \to -1$ which can also be verified from figure 4. The late-time value $\omega_{\rm eff} = -1$ implies that our model converges to ΛCDM model in future. It is also observed that the RDE model does not cross phantom divide line and thus is free from big-rip singularity.

The present value of $\omega_{\rm eff}$ can be found as

$$\omega_{\rm eff}(z = 0) = -1 + \frac{2(\psi_1 - \xi_0)}{\psi_2}. \tag{39}$$

The present value $\omega_{\rm eff}(z = 0) = -0.575$ can be calculated for the best-fit values of parameters. This value is comparatively higher than that predicted by the joint analysis of WMAP + BAO + H_0 + SNe data which is around -0.93.

To calculate the age of the Universe in terms of redshift, we use the definition given by $t(z) = T(z)/H_0$, where

$$T(z) = \int_z^\infty \frac{{\rm d}z'}{(1+z')(H(z')/H_0)}. \tag{40}$$

For the ΛCDM model, the age parameter is [29]

$$T(z) = \int_z^\infty \frac{{\rm d}z'}{(1+z')[\Omega_{m0}(1+z')^3 + (1-\Omega_{m0})]^{1/2}}. \tag{41}$$

We can calculate and plot the age of the Universe with respect to the redshift z using eq. (22) in (40) for the best-fit values as shown in figure 5. The current age of the Universe is found to be $t_0 = 13.397$ Gyr corresponding to the combined SNe + OHD + BAO/CMB data set, which is comparatively the same as predicted by the ΛCDM model.

The fitting achieved from our statistical analysis for the combined data SNe + OHD + BAO/CMB is compatible with the Hubble observational data for the RDE model as shown in figure 6.

Also, the reduced $\chi^2_{\rm red} = \chi^2_{\rm min}/(N - d)$, where N is the number of data and d is the degree of freedom, is calculated for our model and found to be $\chi^2_{\rm red} = 0.77$ which shows that our RDE model provides a very good fit to the considered observational data.

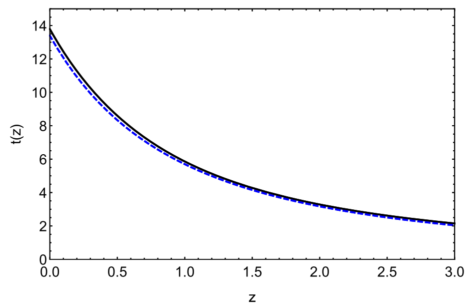

Figure 5. The age of the Universe as a function of redshift where black line represents the age of the ΛCDM model whereas blue dashed line represents the age of the RDE model.

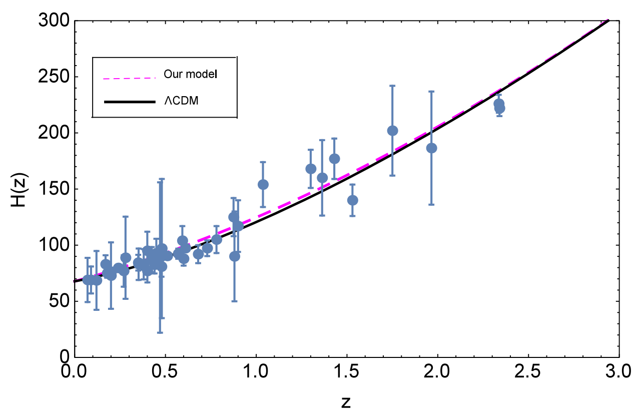

Figure 6. The best-fit curves for the RDE model (dotted magenta) and the ΛCDM model (grey line). The navy blue points with uncertainty bars correspond to the OHD sample.

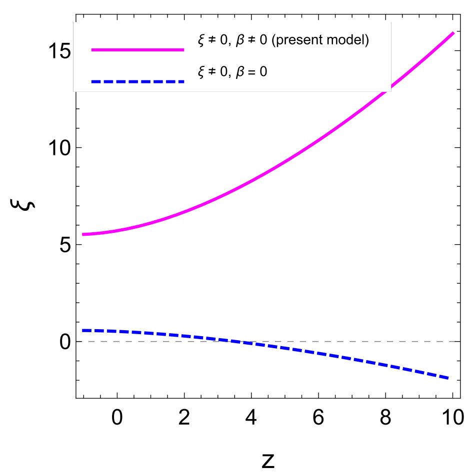

Figure 7. The behaviour of bulk viscous coefficient with redshift for best-fit values of model parameters.

Using (22), we obtain the evolution of bulk viscosity as

$$\xi = \xi_0 + \xi_1 \left[\frac{\xi_0}{\psi_1} + \left(1 - \frac{\xi_0}{\psi_1} \right) (1+z)^{3\psi_1/\psi_2} \right]. \quad (42)$$

The trajectory of bulk viscous coefficient for the best-fit values of model parameters (see table 1) is shown in figure 7. It can be observed that the bulk viscosity is negative at higher redshift (early time) and positive in lower redshift (late time) in the RDE model with bulk viscosity (dotted blue curve). This means that the rate of entropy production is negative in the early epoch and positive in the later epoch. Hence, the entropy law violates in the early epoch and obeys in the later epoch. However, the bulk viscosity decreases at low redshift but always positive in the RDE model with bulk viscosity and matter creation (solid magenta curve). Thus, the model does not violate the law of entropy.

6. Geometrical diagnostics

An important tool for investigating DE model characters nowadays is by the introduction of some geometry quantities, for instance the statefinder diagnostic parameters. Sahni *et al* [88] and Alam *et al* [89] introduced a useful geometrical diagnostic pair $\{r, s\}$, called 'statefinder parameter', which is defined as

$$r = \frac{\dddot{a}}{aH^3} \quad \text{and} \quad s = \frac{r-1}{3(q-1/2)}, \quad (43)$$

where r is the jerk parameter and s is a function of the jerk and the decelerating parameter q. The statefinder parameter pair $\{r, s\}$ of the model concerned is calculated explicitly to demonstrate the behaviour of the RDE model with bulk viscosity and matter creation which is obtained as

$$r = 1 + \frac{9(\xi_0 - \psi_1)\left(1 - \frac{\psi_1}{\psi_2}\right)}{\psi_2 e^{3\xi_0 H_0 (t-t_0)/\psi_2}} + \frac{9(\xi_0 - \psi_1)^2}{\psi_2^2 e^{6\xi_0 H_0 (t-t_0)/\psi_2}} \quad (44)$$

$$s = \frac{\frac{2(\xi_0 - \psi_1)\left(1 - \frac{\psi_1}{\psi_2}\right)}{\psi_2 e^{\frac{3\xi_0 H_0 (t-t_0)}{\psi_2}}} + \frac{2(\xi_0 - \psi_1)^2}{\psi_2^2 e^{\frac{6\xi_0 H_0 (t-t_0)}{\psi_2}}}}{\frac{2(\psi_1 - \xi_0)}{\psi_2 e^{\frac{3\xi_0 H_0 (t-t_0)}{\psi_2}}} - 1}. \quad (45)$$

By using (44) and (45), we plot the r–s plane in figure 8 which shows that the trajectory starts evolving from the region $r > 1, s < 0$, which represents the behaviour of DE with chaplygin gas and evolves through the region $r < 1, s > 0$, which represents the quintessence model of DE and eventually approaches to the point of ΛCDM model represented by the point $\{1, 0\}$. Thus, the RDE model with bulk viscosity and matter creation discriminates with the ΛCDM model in early time. However, the model behaves like the ΛCDM model in the late-time evolution of the Universe.

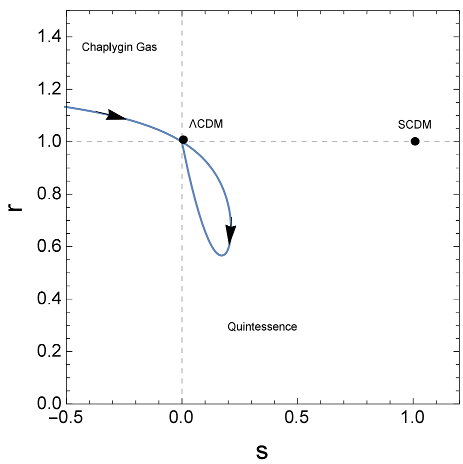

Figure 8. The Universe evolution is diagnostic by the evolution trajectory in the r–s plane for the best-fitted RDE model. The fixed point (0, 1) corresponds to the ΛCDM model. The arrow shows the direction of the evolution of the trajectory.

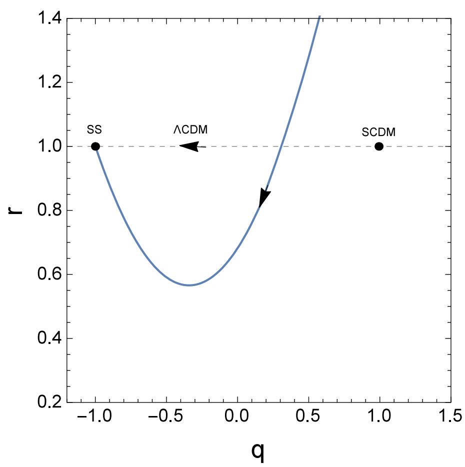

Figure 9. Evolution trajectory in the r–q plane to demonstrate the Universe evolution for the best-fitted RDE model. The horizontal dotted line indicates the ΛCDM model evolution trajectory. The arrow shows the direction of the evolution of the trajectory.

To illustrate more details for the RDE model which is different from the ΛCDM model, we also plot the function trajectory in the r–q plane as shown in figure 9. The dashed line shows the time evolution of the ΛCDM model. The dashed line of the ΛCDM model divides the plane into two parts in which the upper part represents the phantom evolution of the model whereas the lower part represents the non-phantom phase. We can see that the model shows phase transition from deceleration to acceleration as q changes its sign from positive to negative.

To examine the dynamics of the DE models one more diagnostic, called Om, is introduced in [90] with the help of Hubble parameter $H(z)$ and redshift z. It is

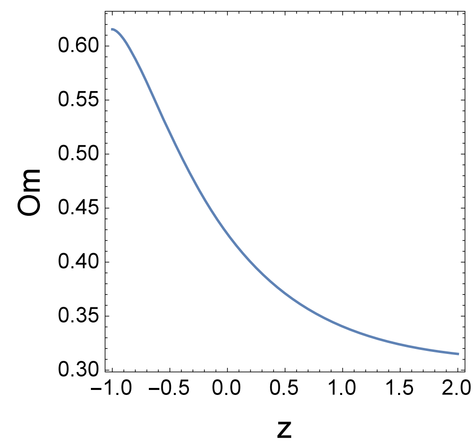

Figure 10. The $Om(z)$–z diagram for the RDE model corresponding to the best-fit parameters.

defined as

$$Om(z) = \frac{(H^2(z)/H_0^2) - 1}{(1+z)^3 - 1}. \tag{46}$$

The Om-diagnostic involves only the first-order derivative of the scale factor. Thus, it is easier to reconstruct from the observational data. The Om-diagnostic is used to check different periods of the Universe. We plot the trajectory in $Om(z)$–z plane to discriminate the behaviour of the DE models. The positive slope of the Om diagnostic means that the model behaves phantom-like while the negative slope indicates the behaviour of quintessence model.

For the RDE model, we obtain

$$Om(z) = \frac{[\xi_0 + (\psi_1 - \xi_0)(1+z)^{3\psi_1/\psi_2}]^2 - \psi_1^2}{\psi_1^2[(1+z)^3 - 1]}. \tag{47}$$

From figure 10, we can observe that the negative slope of the trajectory of $Om(z)$–z plane indicates a behaviour similar to the quintessence model.

To study more about the evolution of the Universe, we expand the scale factor $a(t)$ at $t = t_0$ using Taylor series expansion as

$$a(t) = \sum_{i=0}^{\infty} \frac{a^{(i)}(t_0)}{i!}(t - t_0)^i$$

which provides us some geometrical parameters, known as cosmographic parameters (CP), such as jerk j, snap s and lerk l parameters which can be respectively defined as [91,92]

$$j = \frac{1}{aH^3}\frac{\mathrm{d}^3 a}{\mathrm{d}t^3}, \quad s = \frac{1}{aH^4}\frac{\mathrm{d}^4 a}{\mathrm{d}t^4}, \quad l = \frac{1}{aH^5}\frac{\mathrm{d}^5 a}{\mathrm{d}t^5}. \tag{48}$$

Here r and j are the same; but s defined in (48) is not the same with the one defined in (43). For our model, the variations of parameters j, s and l are discussed by

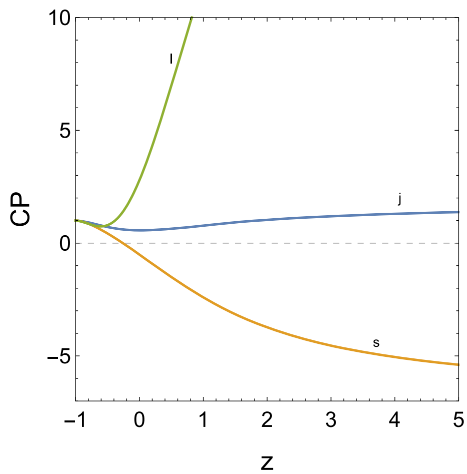

Figure 11. The evolution of the cosmographic parameters jerk j, snap s and lerk l for the best-fit model parameters.

plotting their trajectories against the redshift z as shown in figure 11.

From figure 11, we notice that the jerk parameter remains positive throughout and converges to 1 as z tends to -1 which corresponds to the ΛCDM model. This may indicate that at the present time our model is different from the ΛCDM model but at the late time it converges to the ΛCDM model. The trajectory of s shows the transition from negative to positive, i.e. at the early time s takes the negative value whereas it becomes positive and approaches 1 in the late-time evolution. The trajectory of l remains positive without any transition throughout the evolution and also approaches 1.

7. Energy conditions

In general theory of relativity, the study of singularity theory of space–time was based on energy conditions (ECs). The ECs take the form of various linear combinations of the stress-energy tensor components in such a way that the energy remains positive, or at least non-negative [93]. The famous Raychaudhuri's equation for the expansion nature gives rise to the ECs [94]. Here it is to be noted that the Raychaudhuri's equation is purely geometric and it makes no reference to any gravitational theory under consideration. In FRW Universe, the ECs take the following forms:

$$\text{NEC} \Leftrightarrow \rho_{\text{eff}} + p_{\text{eff}} \geq 0, \quad (49)$$

$$\text{WEC} \Leftrightarrow \rho_{\text{eff}} \geq 0 \;\text{ and }\; \rho_{\text{eff}} + p_{\text{eff}} \geq 0, \quad (50)$$

$$\text{SEC} \Leftrightarrow \rho_{\text{eff}} + 3\,p_{\text{eff}} \geq 0 \;\text{ and }\; \rho_{\text{eff}} + p_{\text{eff}} \geq 0, \quad (51)$$

$$\text{DEC} \Leftrightarrow \rho_{\text{eff}} \geq 0 \;\text{ and }\; \rho_{\text{eff}} \geq |p_{\text{eff}}|, \quad (52)$$

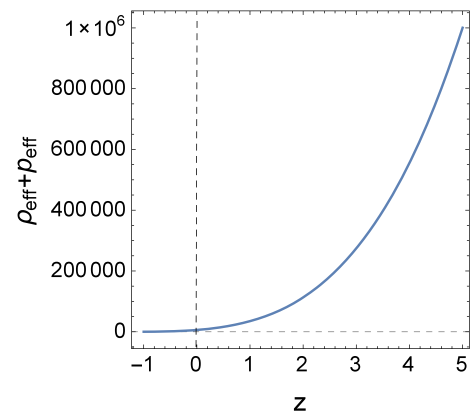

Figure 12. The plot of NEC against z for the best-fit model parameters.

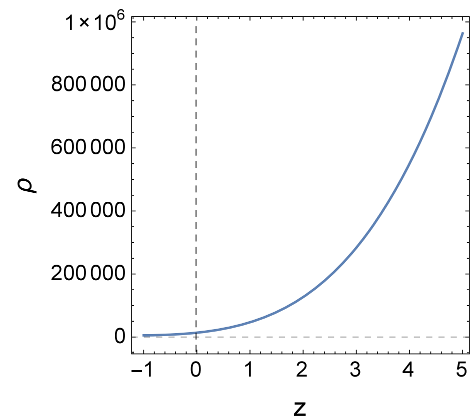

Figure 13. The plot of ρ against z for the best-fit model parameters.

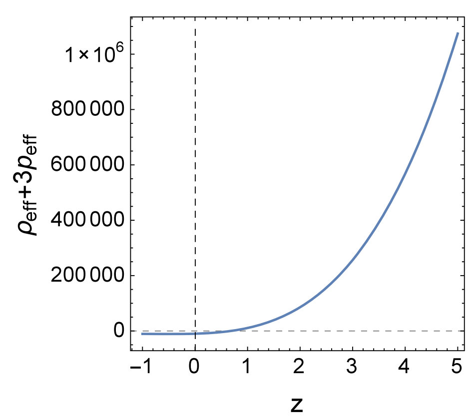

Figure 14. The plot of SEC against z for the best-fit model parameters.

where NEC, WEC, SEC and DEC correspond to the null, weak, strong and dominant energy conditions, respectively. Also in refs [95–97], authors have analysed the ECs in the general theory of relativity.

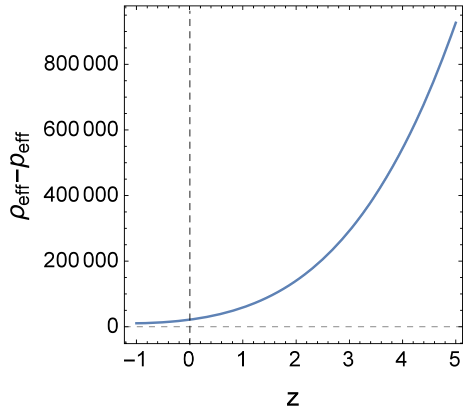

Figure 15. The plot of DEC against z for the best-fit model parameters.

One can observe from figures 12–15 that our model satisfies the NEC, WEC and DEC while it violates the SEC.

8. Conclusion

In the present work, we have discussed the Ricci DE model while considering the effects of bulk viscosity and adiabatic matter creation within the framework of the flat FRW Universe. We have assumed the bulk viscosity coefficient as $\zeta = \zeta_0 + \zeta_1 H$ and the particle creation rate as $\Gamma = 3\beta H$ to obtain exact solutions for the scale factor and various physical quantities. We have considered these two dissipative phenomena as independent irreversible processes. It has been observed that the assumption $\Gamma \propto H$ does not describe the present-day Universe (transition phase) in the absence of bulk viscosity. Also, the RDE model without bulk viscosity and matter creation does not show transition redshift. Therefore, to overcome this problem we have introduced bulk viscosity along with matter creation to observe the present-day Universe and we have succeeded to obtain such a model. We have obtained the Hubble parameter in terms of redshift which is used to obtain the free parameters of the RDE model.

We have performed statistical analysis for our model in §4 using the latest observational data of SNe, OHD and combined data of BAO and CMB. We have employed the publicly available EMCEE codes for implementing the MCMC method. We have obtained the best-fit values for the model parameters (see table 1). Using best-fit values, we have found the transition value of the scale factor ($a_{\rm tr} = 0.936$), the current of the deceleration parameter ($q_0 = -0.362$) and EoS parameter ($\omega_{\rm eff} = -0.575$).

To get further information about the behaviour of the model, we have presented evolution of various cosmological parameters and studied various geometrical diagnostics and cosmographic parameters both analytically and graphically. The deceleration parameter shows a signature flipping behaviour thereby indicating the evolution of the Universe from early deceleration to present late time acceleration (see figure 3). The behaviour of effective EoS parameters (see figure 4) shows that RDE model behaves like de Sitter Universe in late-time of evolution. It has also been observed that the trajectory of $\omega_{\rm eff}$ does not cross phantom divide line and thus is free from big-rip singularity. Figure 5 shows the age of the Universe with respect to redshift z for the best-fit values of the model parameters. The age of the Universe is found to be 13.397 Gyr which is very close to that predicted by the ΛCDM model. From figure 6, it has been observed that these best-fit values of the model parameters are in good agreement with the predictions of the Standard Model. The reduced $\chi^2_{\rm red}$ obtained for the RDE model provides a very good fit to the considered observational data.

Furthermore, we have performed the statefinder diagnostic analysis to this RDE model with bulk viscosity and matter creation to discriminate from the ΛCDM model. In figure 8, we have plotted the r–s trajectory and observed that our model is finally approaching ΛCDM while in figure 9 there is a sign change of q from positive to negative which shows that our model changes the phase from deceleration to acceleration. In both the figures arrows show the direction of the trajectories in the plane. The Om diagnostic which is obtained from the Hubble parameter shows the negative slope in $Om(z)$–z plane trajectory (figure 10), i.e. its behaviour is similar to the quintessence model. We have also discussed cosmographic parameters like j, s, l to compare our model with the ΛCDM model. From figure 11, we can observe from the trajectory of jerk j that at present our model is different from the ΛCDM model but in the late time it converges to ΛCDM. We can observe from the trajectory of s that it changes its sign from negative to positive during the evolution and finally converges to 1. Similarly, l shows no transition with respect to z and reaches 1 in the late future.

Finally, we have examined the ECs of our model to analyse the physical viability of the model. It has been observed from figures 12–15 that our model satisfies NEC, WEC and DEC but it violates the SEC.

Acknowledgements

One of the author, AK would like to thank University Grants Commission, New Delhi for providing Senior Research Fellowship under UGC-NET Scholarship.

References

[1] A G Riess *et al*, *Astron. J.* **116**, 1009 (1998)
[2] S Perlmutter *et al*, *Nature* **391**, 51 (1998)
[3] S Perlmutter *et al*, *Astrophys. J.* **517**, 565 (1999)
[4] K Bamba, S Capozziello, S Nojiri and S D Odintsov, *Astrophys. Space Sci.* **342**, 155 (2012)
[5] M Li, X D Li, S Wang and Y Wang, *Commun. Theor. Phys.* **56**, 525 (2011)
[6] B Wang, E Abdalla, F Atrio-Barandela and D Pavon, *Rep. Prog. Phys.* **79(5)**, 096901 (2016)
[7] P J E Peebles and B Ratra, *Rev. Mod. Phys.* **75**, 559 (2003)
[8] E J Copeland, M Sami and S Tsujikawa, *IJMPD* **15**, 1753 (2006)
[9] J A Frieman, M S Turner and D Huterer, *Annu. Rev. Astron. Astrophys.* **46**, 385 (2008)
[10] R R Caldwell and M Kamionkowski, *Annu. Rev. Astron. Astrophys.* **59**, 397 (2009)
[11] M Li, X D Li, S Wang and Y Wang, *Front. Phys.* **8**, 828 (2013)
[12] T Padmanabhan, *Phys. Rep.* **380**, 235 (2003)
[13] V Sahni and A Starobinsky, *Int. J. Mod. Phys. D* **9**, 373 (2000)
[14] R Bousso, *Rev. Mod. Phys.* **74**, 825 (2002)
[15] M Li, *Phys. Lett. B* **603**, 1 (2004)
[16] W Fischler and L Susskind, arXiv:hep-th/9806039
[17] Y Gong, *Phys. Rev. D* **70**, 064029 (2004)
[18] B Wang, Y Gong and E Abdalla, *Phys. Lett. B* **624**, 141 (2005)
[19] X Zhang, *Int. J. Mod. Phys. D* **14**, 1597 (2005)
[20] D Pavon and W Zimdahl, arXiv:hep-th/0511053
[21] A G Cohen *et al*, *Phys. Rev. Lett.* **82**, 4971 (1999)
[22] C Gao, F Wu and X Chen, *Phys. Rev. D* **79**, 043511 (2009)
[23] C J Feng, *Phys. Lett. B* **670**, 231 (2008)
[24] M Bouhmadi-López and Y Tavakoli, *Phys. Rev. D* **87**, 023515 (2013)
[25] M Suwa, K Kobayashi and H Oshima, *J. Mod. Phys.* **6**, 327 (2015)
[26] S Ghaffari, A Sheykhi and M H Dehghani, *Phys. Rev. D* **91**, 023007 (2015)
[27] C W Misner, *Astrophys. J.* **151**, 431 (1968)
[28] Y D Xu, Z G Huang and X H Zhai, *Astrophys. Space Sci.* **337**, 493 (2012)
[29] C J Feng and X Z Li, *Phys. Lett. B* **680**, 355 (2009)
[30] S Nojiri and S D Odintsov, *Phys. Rev. D* **72**, 023003 (2005)
[31] S Capozziello *et al*, *Phys. Rev. D* **73**, 043512 (2006)
[32] N Cruz, S Lepe and F Pena, *Phys. Lett. B* **646**, 177 (2007)
[33] J Ren and X H Meng, *Phys. Lett. B* **633**, 1 (2006)
[34] M G Hu and X H Meng, *Phys. Lett. B* **635**, 186 (2006)
[35] P Kumar and C P Singh, *Astrophys. Space Sci.* **357**, 120 (2015)
[36] C P Singh, *Pramana – J. Phys.* **71**, 33 (2008)
[37] C P Singh, S Kumar and A Pradhan, *Class. Quantum Grav.* **24**, 455 (2007)
[38] C P Singh and P Kumar, *Eur. Phys. J. C* **74**, 3070 (2014)
[39] C P Singh and Milan Srivastava, *Eur. Phys. J. C* **78**, 190 (2018)
[40] Milan Srivastava and C P Singh, *Astrophys. Space Sci.* **363**, 117 (2018)
[41] C P Singh and A Kumar, *Eur. Phys. J. Plus* **133**, 312 (2018)
[42] C P Singh and Amit Kumar, *Astrophys. Space Sci.* **364**, 94 (2019)
[43] C P Singh and Simran Kaur, *Astrophys. Space Sci.* **365**, 2 (2019)
[44] I Prigogine *et al*, *Proc. Natl. Acad. Sci. USA* **85**, 7428 (1988)
[45] I Prigogine *et al*, *Gen. Relativ. Gravit.* **21**, 8 (1989)
[46] J A S Lima, M O Calvão and I Waga, in *Frontier physics, Essays in honor of Jayme Tiomno* (World Scientific, Singapore, 1990)
[47] M O Calvão, J A S Lima and I Waga, *Phys. Lett. A* **162**, 223 (1992)
[48] J A S Lima and A S M Germano, *Phys. Lett. A* **170**, 373 (1992)
[49] W Zimdahl and D Pavón, *Mon. Not. R. Astron. Soc.* **266**, 872 (1994)
[50] J A S Lima, A S M Germano and L R W Abramo, *Phys. Rev. D* **53**, 4287 (1996)
[51] J S Alcaniz and J A S Lima, *Astron. Astrophys.* **349**, 729 (1999)
[52] W Zimdahl, D J Schwarz, A B Balakin and D Pavón, *Phys. Rev. D* **64**, 063501 (2001)
[53] J A S Lima, F E Silva and R C Santos, *Class. Quant. Grav.* **25**, 205006 (2008)
[54] T Harko and F S N Lobo, *Phys. Rev. D* **87**, 044018 (2013)
[55] S Basilakos and M Plionis, *Astron. Astrophys.* **507**, 47 (2009)
[56] G Steigman, R C Santos and J A S Lima, *J. Cosmol. Astropart. Phys.* **06**, 033 (2009)
[57] J A S Lima, J F Jesus and F A Oliveira, *J. Cosmol. Astropart. Phys.* **11**, 027 (2010)
[58] S Basilakos and J A S Lima, *Phys. Rev. D* **82**, 023504 (2010)
[59] C P Singh and A Beesham, *Astrophys. Space Sci.* **336**, 469 (2011)
[60] C P Singh, *Astrophys. Space Sci.* **338**, 411 (2012)
[61] S Chakraborty, S Pan and S Saha, *Phys. Lett. B* **738**, 424 (2014)
[62] S Pan and S Chakraborty, *Adv. High Energy Phys.* **15**, 654025 (2015)
[63] J Haro and S Pan, *Class. Quantum Gravit.* **33**, 165007 (2016)
[64] C P Singh and Simran Kaur, *Phys. Rev. D* **100**, 084057 (2019)
[65] C P Singh and Ajay Kumar, *Eur. Phys. J. C* **80**, 106 (2020)
[66] D Pavon, J Gariel and G Le Denmat, *Gen. Relativ. Gravit.* **28**, 573 (1996)
[67] I Brevik and G Stokka, *Astrophys. Space Sci.* **239**, 89 (1996)

[68] C P Singh, *Mod. Phys. Lett. A* **27**, 1250070 (2012)
[69] R Sudarsan and V P Johri, *Gen. Relativ. Gravit.* **26**, 41 (1994)
[70] J Triginer and D Pavón, *Gen. Relativ. Gravit.* **26**, 513 (1994)
[71] C Eckart, *Phys. Rev.* **58**, 919 (1940)
[72] X H Meng, J Ren and M G Hu, *Commun. Theor. Phys.* **47**, 379 (2007)
[73] X H Meng and X Dou, *Commun. Theor. Phys.* **52**, 377 (2009)
[74] A Avelino and U Nucamendi, *J. Cosmol. Astropart. Phys.* **08**, 009 (2010)
[75] D Foreman-Mackey, D W Hogg, D Lang and J Goodman, *PASP* **125**, 306 (2013)
[76] P A R Ade *et al*, *Astron. Astrophys.* **594**, 13 (2016)
[77] M Betoule *et al*, *Astron. Astrophys.* **568**, A22 (2014), arXiv:1401.4064 [astro-ph.CO]
[78] S L Cao *et al*, *The Eur. Phys. J. C* **78**, 170 (2018)
[79] M V dos Santos, R R R Reis and I Waga, *J. Cosmol. Astropart. Phys.* **02**, 066 (2016)
[80] N Padmanabhan *et al*, *Mon. Not. R. Astron. Soc.* **427**, 2132 (2012)
[81] F Beutler *et al*, *Mon. Not. R. Astron. Soc.* **416**, 3017 (2011)
[82] L Anderson *et al*, *Mon. Not. R. Astron. Soc.* **441**, 24 (2014)
[83] C Blake *et al*, *Mon. Not. R. Astron. Soc.* **425**, 405 (2012)
[84] P A R Ade *et al*, Planck 2015 results. XIII. Cosmological parameters, Preprint arXiv:1502.01589 (2015)
[85] G Hinshaw *et al*, *Astrophys. J. Suppl. Ser.* **208**, 19 (2013)
[86] WMAP Collabration: G Hinshaw *et al*, *Astrophys. J. Suppl.* **180**, 225 (2009)
[87] U Alam, V Sahni and A A Starobinsky, *J. Cosmol. Astropart. Phys.* **0406**, 008 (2004)
[88] V Sahni, T D Saini, A A Starobinsky and U Alam, *JETP Lett.* **77**, 201 (2003)
[89] U Alam *et al*, *Mon. Not. R. Astron. Soc.* **344**, 1057 (2003)
[90] V Sahni, A Shaleloo and A A Starobinsky, *Phys. Rev. D* **78**, 103502 (2008)
[91] M Visser, *Class. Quant. Gravit.* **21**, 2603 (2004)
[92] M Visser, *Gen. Relativ. Gravit.* **37**, 1541 (2005)
[93] M Visser and C Barcelo, *COSMO-99*, 98 (2000), arXiv:gr-qc/0001099
[94] S Carroll, *Spacetime and geometry: An introduction to general relativity* (Addison Wesley, Boston, 2004)
[95] J Santos and J S Alcaniz, *Phys. Lett. B* **619**, 11 (2005)
[96] J Santos *et al*, *Phys. Rev. D* **76**, 043519 (2007)
[97] A A Sen and R J Scherrer, *Phys. Lett. B* **659**, 457 (2008)